

Hand-Held Personal Laser Scanning – Current Status and Perspectives for Forest Inventory Application

Ivan Balenović, Xinlian Liang, Luka Jurjević, Juha Hyyppä, Ante Seletković, Antero Kukko

Abstract

The emergence of hand-held Personal Laser Scanning (H-PLS) systems in recent years resulted in initial research on the possibility of its application in forest inventory, primarily for the estimation of the main tree attributes (e.g. tree detection, stem position, DBH, tree height, etc.). Research knowledge acquired so far can help to direct further research and eventually include H-PLS into operational forest inventory in the future. The main aims of this review are:

- ⇒ to present the current state of the art for H-PLS systems
- ⇒ briefly describe the fundamental concept and methods for H-PLS application in forest inventory
- ⇒ provide an overview of the results of previous studies
- ⇒ emphasize pros and cons for H-PLS application in forest inventory in relation to conventional field measurements and other similar laser scanning systems
- ⇒ highlight the main issues that should be covered by further H-PLS-based forest inventory studies.

Keywords: Hand-held Personal Laser Scanning (H-PLS), LiDAR, forest inventory, individual-tree-based approach (ITD), tree detection, stem position, diameter at breast height (DBH), tree height

1. Introduction

The potential of remote sensing application in forest inventory has long been recognized by both forest science and practice (White et al. 2016). In recent decades, the most significant progress in remote-sensing-based forest inventory studies has resulted from the development of laser scanning (LS) technology also known as light detection and ranging (LiDAR) (Wang et al. 2019). LS is an active remote sensing technology for collecting high-precision three-dimensional (3D) spatial data (point cloud) based on laser scanning, ranging, positioning and orientation measurement techniques (Petrie and Toth 2009). According to Wang et al. (2019), the main advantages of LS technology in forest inventory are:

- ⇒ direct acquisition of 3D attributes of objects (trees)
- ⇒ capability of canopy penetration, which enables the detection of tree tops, the terrain and vertical forest structure in single data acquisition
- ⇒ a high level of automation in data processing, which facilitates efficient measurements over large areas.

Based on the platforms on which the system is mounted, the LS technology is grouped into space-borne, airborne, and unmanned aircraft systems, mobile, personal, and terrestrial systems. Each system provides data of certain characteristics that could serve for specific forest inventory needs, at individual branch-, tree-, plot-, stand-, country- and global-level.

There are two main approaches to derive forest inventory data from LS: the area-based approach (ABA) and the individual-tree-based approach (ITD). Currently, only Airborne Laser Scanning (ALS) based on ABA is implemented in operational forest inventory in a number of countries (Næsset 2014, Tuominen et al. 2014, Ørka et al. 2018, Wang et al. 2019). The ABA uses point cloud metrics and field reference data of a certain number of sample plots to establish prediction models that are further used solely with point cloud metrics to estimate forest attributes at plot- and stand-level (wall-to-wall mapping) for a wider, targeted area. The ITD uses point cloud to detect, segment and model individual trees and to extract individual-tree attributes. Therefore, direct ITD measurements of tree attributes require point clouds of high density describing the geometry of a tree.

LS technology changes the forest inventories in many perspectives. Among them, applying terrestrial and mobile LS systems in field inventories in order to reduce labor-intensive and time-consuming field work has received a lot of attention. The first studies on the possibilities of applying Terrestrial Laser Scanning (TLS) in forest inventory started around 2000. During the last decade, this topic has been more intensively studied (Liang et al. 2012, 2014, Bauwens et al. 2016, Cabo et al. 2018, Liang et al. 2018a), i.e. when TLS hardware underwent considerable improvements in terms of decreased size, weight and price, and increased spatial resolution and measurement speed (Liang et al. 2018a). By applying TLS in forest inventories, individual trees and forest plots can be digitized in detail at millimeter-level that further enables accurate extraction or estimation of the main tree attributes, such as position, diameter at breast height (DBH), tree height, stem curve, volume, aboveground biomass, etc (Bauwens et al. 2016, Cabo et al. 2018, Liang et al. 2018a). The main limitation of TLS that hinders its operational use in forest inventory is the speed of data acquisition. Namely, to reduce the occlusion effect caused by surrounding trees, each plot needs to be scanned from multiple positions using multi- or multi-single-scan approach, which is time-consuming and costly.

Mobile Laser Scanning (MLS) systems present time-efficient alternative to TLS because they can reduce occlusion problem and acquisition time. Apart from the platform (vehicle or human), MLS systems typically consist of three main components:

- ⇒ laser scanner (LiDAR sensor)
- ⇒ inertial measurement unit (IMU)
- ⇒ Global Navigation Satellite System (GNSS) receiver.

The quality and accuracy of the MLS data depend on the precision and accuracy of all three components and their synchronization (Bauwens et al. 2016). Due to the degraded GNSS signal in the forest environment and dynamics of the moving platform observed by IMU, MLS data are usually less accurate than TLS data (Liang et al. 2018b). Furthermore, vehicles have limited access to certain, more complex forest areas, which prevents continuous moving and data acquisition. This moving limitation in the forest has motivated the use of human-operator as a platform, where all sensors are carried by a human operator, also referred to as Personal Laser Scanning (PLS). The first PLS systems were large in size and heavy in weight (30+ kg) (Kukko et al. 2012, Hyypä et al. 2013, Liang et al. 2014). During the last years, rapid progress in sensor miniaturization resulted in the development of lightweight and highly mobile hand-held PLS (H-PLS) systems. Further progress in H-PLS systems was achieved by replacing GNSS with Simultaneous Localization and Mapping (SLAM) algorithm. SLAM algorithm processes IMU and laser data to locate the scanner in an unknown environment and to register the whole point cloud, making H-PLS systems suitable for use in the forest where the GNSS signal is often degraded. In literature, various terms were used for H-PLS systems, such as hand-held Mobile Laser Scanning (HMLS), hand-held Laser Scanning (HLS), Wearable Laser Scanning (WLS) or just Personal Laser Scanning (PLS) (Gollob et al. 2020).

The emergence and availability of H-PLS systems in recent years resulted in an initial research on the possibility of its application in forest inventory, primarily for the estimation of the main tree attributes (e.g. stem position, DBH, tree height, etc.). Although a limited number of studies have been conducted up to now, knowledge acquired so far can help to direct further research and eventually include H-PLS into forestry practice. The main objectives of this paper are:

- ⇒ to present the current state of the art of H-PLS systems
- ⇒ briefly describe the fundamental concept and methods for H-PLS application in ITD forest inventory
- ⇒ provide an overview of the results of previous studies
- ⇒ emphasize pros and cons for H-PLS application in forest inventory in relation to other similar LS systems (e.g. TLS, MLS)
- ⇒ highlight the main issues that should be covered by further H-PLS-based forest inventory studies.

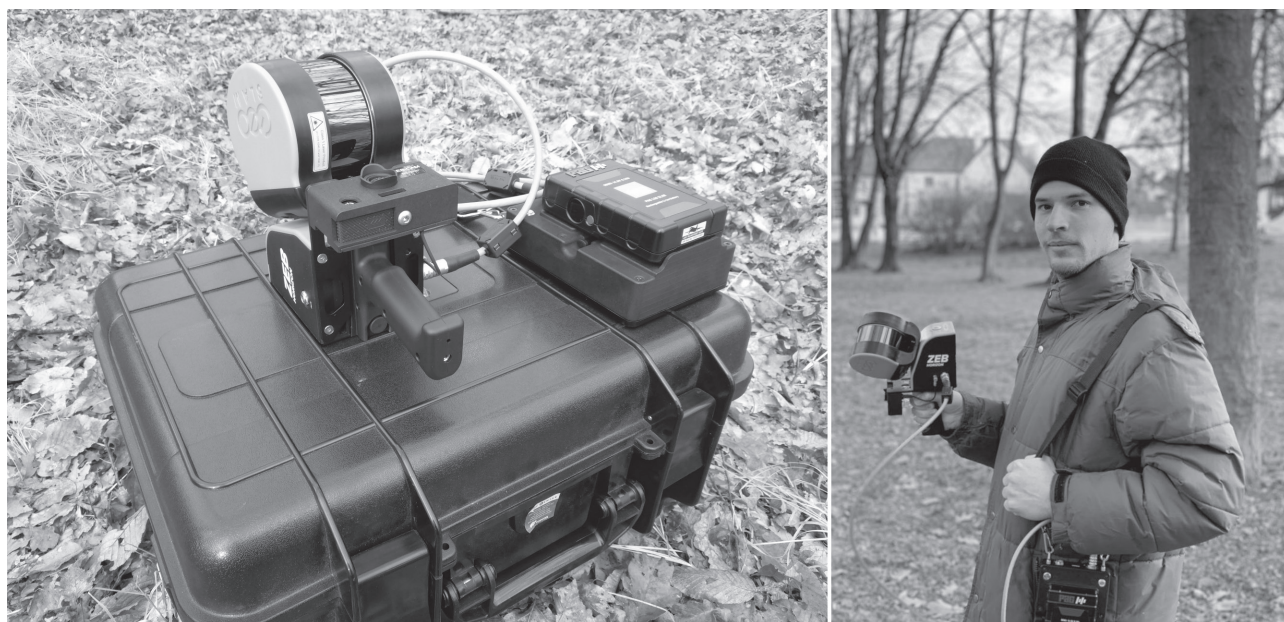


Fig. 1 ZEB-HORIZON instrument

Table 1 Technical specifications of contemporary commercial H-PLS systems already used or with potential to be used in forest inventory

Feature	ZEB1	ZEB-REVO (ZEB-REVO-RT1)	ZEB HORIZON	PX-80	HERON LITE Color	BLK2GO	STENCIL 2-32
Launched, year	2013	2015 (2017)	2019	2019	–	–	–
Laser scanner	UTM-30LX	UTM-30LX-F	VLP-16	VLP-16	VLP-16 LW	–	HDL-32
Maximum range, m	30 (15–20 outdoor)	30 (15–20 outdoor)	100	100	100	25	100
Range accuracy, cm	3	1–3	1–3	1–3	–	–	2
Acquisition rate points·sec ⁻¹	43,200	43,200	300,000	300,000	300,000	420,000	720,000
Number of sensors	1	1	16	16	16	2	32
Scanner resolution: horizontal, ° / vertical, °	0.625/1.8	0.625/1.8	0.1–0.4/2	–	0.1–0.4/2	–	0–1–0.4
Field of View: horizontal, ° / vertical, °	270/120	270/360	270/360	360/30 (± 15)	360/30 (± 15)	360/270	360/40 (+ 10.67/–30.67)
Wavelength, nm	905	905	903	903	903	830	903
Scanner line speed, Hz	40	100	5–20	–	5–20	–	10
Beam Divergence, mrad	1.7x14	1.7x14	3.0	3.0	3.0	–	–
Camera	ZEB-CAM	ZEB-CAM	ZEB-CAM	Spherical camera	360° Camera	Panoramic camera	Panoramic camera
Scanner weight, kg	0.7 (665 g)	1 (850 g)	1.3	–	2.75	0.65	–
Total weight, kg	–	4.1	3.7	2.9	4.15	0.775	2.200

1 ZEB-REVO-RT instrument is the successor of ZEB-REVO. Both instruments consist of the same type of sensors and have the same technical characteristics. The only difference is that ZEB-REVO-RT is capable of real time-data processing and visualization

2. H-PLS Sensors and Systems

Recently, a number of commercial H-PLS systems have become available on the market with the primary application for indoor scanning. Meanwhile, the performance of several H-PLS systems (ZEB1, ZEB-REVO, ZEB-REVO-RT, ZEB-HORIZON) was evaluated in forest conditions as well (Fig. 1, Table 1).

Compared to high-end backpack PLS in the sense of size, weight and sensor performance, H-PLS systems typically consist of low-cost LiDAR sensors and low-accuracy Micro-Electrical Mechanical Systems (MEMS) IMUs facilitating handheld operation. GNSS receiver is usually not integrated in such systems. Table 1 shows the technical characteristics of contemporary commercial H-PLS systems. It can be noted that most recently launched H-PLS systems (ZEB-HORIZON, PX-80, HERON-LITE) consist of VLP-16 LiDAR sensor; a low-cost sensor primarily used for navigation purposes. Compared to the UTM-30LX sensor incorporated in the first H-PLS systems (ZEB1, ZEB-REVO), the use of VLP-16 has considerably improved the scanning range (up to 100 m) and acquisition rate (300,000 points per second). However, range accuracy is moderate in 3 cm range and beam divergence is fairly large (3–5 mrad), which both adversely affect the localization uncertainty of individual points.

Despite the capability of such sensors to collect a large amount of points, the resulting data are still of significantly lower quality than data collected with the contemporary TLS. Namely, compared to TLS data, the H-PLS data have a significantly lower point den-

sity, ranging accuracy and angular resolution, while beam divergence and resulting footprint are significantly larger. For example, the manufacturer's declared accuracy of VLP-16 LiDAR sensor is ± 3 cm in »typical« conditions, whereas beam divergence is 3 mrad, resulting in footprint of 7.5 cm in the range of 25 m. For the reference, the accuracy of the contemporary TLS is ± 2 mm at 25 m, whereas beam divergence is ~ 0.1 mrad, resulting in footprint of 2.5 mm in range of 25 m. In summary, TLS laser beam has 10–20 higher resolutions than H-PLS based on these parameters. Fig. 2 shows a comparison of multi-scan TLS (FARO 70S scanner) and H-PLS (ZEB-HORIZON) data, where it can be seen that H-PLS data has substantially more noise and less details compared to TLS.

Since H-PLS systems usually do not have GNSS receiver to provide absolute positioning, H-PLS point clouds are usually produced in the local coordinate frame, which can be further georeferenced, i.e. rotated and translated to a global geographical coordinate system in post-processing. Both TLS and H-PLS point clouds are commonly georeferenced using precisely measured features that are easy to detect in the point cloud, such as spheres of known diameter and position (map coordinates) (Fig. 3). To precisely georeference the scan, at least three spheres must be placed in the scanning area, where the positions of the spheres have to be measured with high accuracy using a total station or a GNSS receiver. This step is a necessity when analyzing multi-source or multitemporal data in e.g. growth estimations, though some of the H-PLS systems provide modes for (real-time) scan matching based on existing point cloud/map.

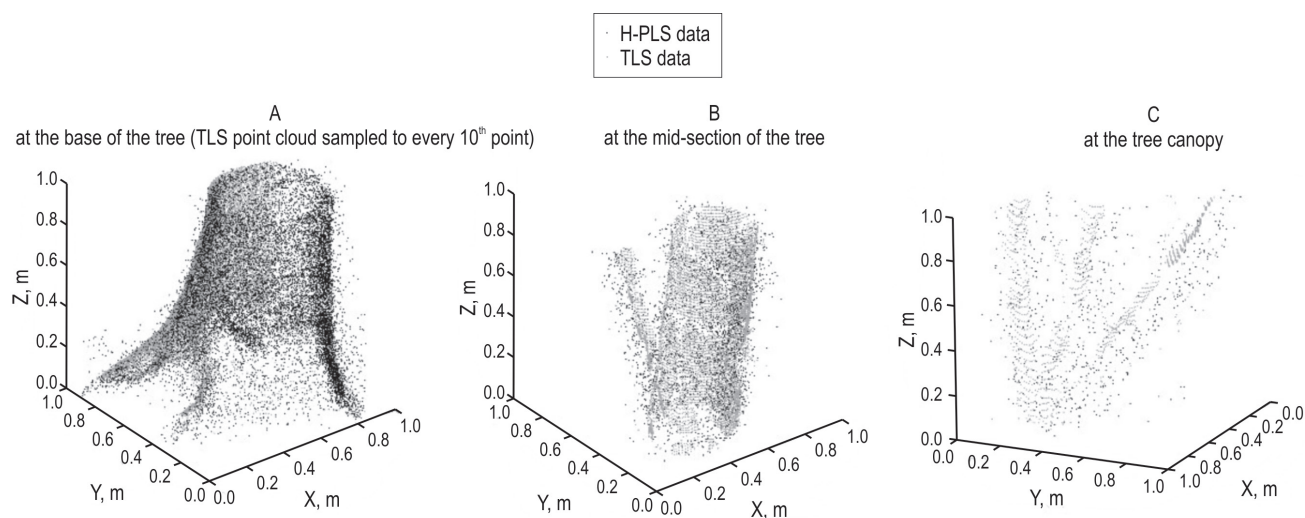


Fig. 2 Comparison of H-PLS (ZEB-HORIZON) and TLS (FARO 70S scanner) point clouds



Fig. 3 Sphere placed in forest inventory plot to georeference TLS point cloud

3. H-PLS in Forest Inventory Research

The increased interest in H-PLS in forest application can be noticed during the last two years (Table 2), despite the limited number of conducted and published studies. Among various observed individual tree attributes, the extraction and estimation of DBH using H-PLS data (point cloud) attracted the attentions almost in all of the previous studies. Attentions were also given to tree detection (TD) and extraction of tree position (TP), followed by tree height (H) estimation and time/work efficiency (EFF) assessment. Other attributes (variables) were also examined, e.g., crown base height (CBH) and crown projection area radii (CPAR), as well as different walking scan paths using H-PLS for the estimation of individual tree attributes.

It can be noticed that, out of all currently available H-PLS instruments (Table 1), only four different instruments have so far been tested in forest inventory studies, and most of them are from the same manufacturer (GeoSLAM Ltd.). Zhou et al. (2019) used a home-designed instrument, where the system used VLP-16 LIDAR sensor that is common in the most recently

launched H-PLS systems (ZEB-HORIZON, PX-80, HERON-LITE).

Prior to any comparison of the results obtained, it should be emphasized that different validation approaches in H-PLS inventory studies were used, i.e. H-PLS data were compared and evaluated using different reference (ground-truth) data. While in most studies, conventional field measurements were used as ground-truth data (Bauwens et al. 2016, Gianneti et al. 2018, Oveland et al. 2018, Chen et al. 2019, Zhou et al. 2019, Gollob et al. 2020, Vantadaşlar et al. 2020, Jurjević et al. 2020), in several studies H-PLS data were evaluated using TLS data (Ryding et al. 2015, Cabo et al. 2018). Hyypä et al. (2020a) mainly focused on deriving stem volume from the H-PLS system based on stem curve and tree height information.

This section further provides an overview of the results of previous studies with a special emphasis on each individual tree attribute.

3.1 Data Collection (Scanning Approach) and Time/Work Efficiency

In general, data collection with H-PLS instruments usually encompasses the following main steps:

- ⇒ IMU initialization – to establish the local coordinate system
- ⇒ scanning – by an operator walking. Collected data are stored in real-time on the hard drive of data logger connected to the scanner via cable
- ⇒ position measurements of spheres – using a total station or GNSS receiver. This step is required only if georeferenced data are needed
- ⇒ point cloud processing – data transfer and automatic registration with the SLAM algorithm using accompanying software, georeferencing of the registered point cloud, and finally extraction of variables of interest (e.g. tree location, DBH, tree height, etc.) using the appropriate software.

Data collection in forest inventory using H-PLS systems is usually performed by an operator walking along the planned scan path throughout the study area (e.g. sample plots). The walking scan path has to be carefully planned because it directly influences the performance of the SLAM algorithm, and consequently the quality of collected data (density and quality of the point cloud) and the accuracy of individual tree estimates. The first factor to be considered when planning a walking scan path is the forest conditions, similarly in all mobile systems (Liang et al. 2018b). In H-PLS, particular attention has to be paid on the range of the laser instrument. In addition, acquisition time

Table 2 Summary of conducted H-PLS-based forest inventory studies

Study	Location	Forest type; Dominant tree species	Surveyed area	Stem density steems · ha ⁻¹	H-PLS instrument	Observed attributes variables				
						TD	TP	DBH	H	EFF
Ryding et al. (2015)	UK	Semi-natural forest with dense understorey; <i>Fraxinus excelsior</i>	3 plots (10×10 m)	n.a.	ZEB1	✓	✓	✓	–	✓
Bauwens et al. (2016)	Belgium	Broadleaf forests (coppice, even-aged, uneven-aged); <i>Fagus sylvatica</i> , <i>Carpinus betulus</i> , <i>Betula</i> spp.	5 plots (r=15 m)	113–835	ZEB1	✓	✓	✓	–	✓
		Conifer forests (even-aged) forests; <i>Picea abies</i> , <i>Pseudotsuga menziessi</i>	4 plots (r=15 m)	113–1344	ZEB1	✓	✓	✓	–	✓
		Mixed (even-aged) forests; <i>Quercus</i> spp., <i>Pinus sylvestris</i>	1 plot (r=15 m)	439	ZEB1	✓	✓	✓	–	✓
Cabo et al. (2018)	Spain	Site A) Urban pine forest (mixed two-aged stand); <i>P. pinea</i> , <i>Platanus hispanica</i>	one single area (1 ha)	n.a.	ZEB-REVO	✓	✓	✓	✓	–
		Site B) Mountain pine forest (even-aged, pure stand); <i>P. sylvestris</i>	one single area (0.5 ha)	n.a.	ZEB-REVO	✓	✓	✓	✓	–
Gianneti et al. (2018)	Italy	Mediterranean multi-layered forest; <i>Cupressus sempervirens</i> , <i>P. pinaster</i> , <i>Quercus ilex</i>	1 plot (r=13 m)	106	ZEB1	✓	✓	✓	✓	–
Oveland et al. (2018)	Norway	Boreal forest; <i>P. abies</i> , <i>P. sylvestris</i> , <i>B. pubescens</i> , <i>Larix deciduae</i> , <i>Abies alba</i>	7 plots (r=12.6 m)	967 (380–1380)	ZEB1	✓	✓	✓	–	✓
Chen et al. (2019)	China	Arbor, artificial forest; <i>Styphnolobium japonicum</i> , <i>Sophora japonica</i> , <i>Betula</i> spp., <i>P. armandii</i>	1 plot (15×20 m)	1100	ZEB-REVO-RT	✓	✓	✓	–	✓
Del Perugia et al. (2019)	Italy	Pure culture stand; <i>Castanea sativa</i>	3 circular plots (r=30 m)	110	ZEB1	✓	✓	✓	✓	✓
Zhou et al. (2019)	China	Urban park forest; Eucalyptus and poplar trees	One single area (perimeter=130 m)	n.a.	Self-made Velodyne VLP-16	–	–	✓	–	–
Vantadaşlar and Zeybek (2020)	Turkey	Various types of pure and mixed temperate forests; <i>P. orientalis</i> , <i>P. sylvestris</i> , <i>F. orientalis</i> , etc.	9 plots of different shapes and sizes	505 (200–1225)	ZEB-REVO	–	–	✓	–	–
Gollob et al. (2020)	Austria	Various forest types (broadleaved, coniferous, mixed), forest structure (one- or two-layered) and terrain characteristics	20 circular plots (r=20 m)	981 (239–3350)	ZEB-HORIZON	✓	–	✓	–	–
Hyppä et al. (2020a)	Finland	Boreal, coniferous-dominated, mixed stands (1 plot in sparse and 1 in obstructed stand)	2 plots (32×32 m)	410, 420	ZEB-HORIZON	✓	–	✓	✓	–
Jurjević et al. (2020)	Croatia	Lowland (even-aged) deciduous forest; <i>Quercus robur</i>	6 plots (r=15 m)	305	ZEB-HORIZON	–	–	–	✓	–
Vantadaşlar and Zeybek (2020)	Turkey	Various types of pure and mixed temperate forests; <i>P. orientalis</i> , <i>P. sylvestris</i> , <i>F. orientalis</i> , etc.	9 plots of different shapes and sizes	505 (200–1225)	ZEB-REVO	–	–	✓	–	–

TD – Tree Detection; TP – Tree Position; DBH – Diameter at Breast Height; H – Tree Height; EFF – Time/Work efficiency

and costs are also important factors for an efficient survey.

In previous studies, different scanning paths were applied and tested. Ryding et al. (2015) applied a free walking method forming a closed loop by starting and ending the survey at the same point (Fig. 4a). The survey for each plot (10×10 m) was completed in less than five minutes, including time spent for the initialization of the system at the beginning and end of each scan.

Bauwens et al. (2016) designed the scanning path where the sample plots were circular ($r=15$ m). The survey ends at the starting point. The plots were crossed four times, and the plot border was passed at least once and sometimes twice (Fig. 4b) to the aim of the scan path to (i) obtain appropriate distribution of scanning positions that will ensure coverage of all trees and high scanning density; (ii) reduce scanner range noise; (iii) avoid problems associated with drift, which can occur when the SLAM algorithm fails to register scans correctly. The total time spent for the H-PLS survey per plot was 24 min, including 11 min for the setting up (preparation and initialization of the scanner) and 13 min for the scanning. Data processing by an experienced person was completed in 1 h and 46 min.

Gianneti et al. (2018), Oveland et al. (2018) and Gollob et al. (2020) applied a similar scanning approach as proposed by Bauwens et al. (2016) to scan circular sample plots ($r=13$ m, $r=12.6$ m, and $r=20$ m, respectively). Oveland et al. (2018) reported time consumption for H-PLS scanning without positioning (24 min per plot) similar to Bauwens et al. (2016).

To georeference the PCs, Gianneti et al. (2018) used six spherical targets placed on the ground at different cardinal positions and distances from the plot center to georeference the PC in post-processing. The high-precision measurement of the spherical targets using the GNSS receiver lasted approximately 20 min. Oveland et al. (2018) placed three spherical targets within each plot, whose positions were measured using a total station from the plot center, with an additional time consumption of approximately 5 min. Opposite to the above studies, Gollob et al. (2020) did not use and measure spheres. For 20 surveyed plots, Gollob et al. (2020) reported a scanning time of 7–15 min per plot, which depended on the possible walking speed, i.e. on forest and terrain characteristics.

To obtain maximum coverage of all trees and high-resolution point cloud for the rectangular plot (15×20 m), Chen et al. (2019) applied the serpentine scanning approach by slow walking (Fig. 4c) that lasted approxi-

mately 5 min including 15 seconds for system initialization.

Vantadaşlar and Zeybek (2020) used a simple scanning approach for H-PLS survey of 9 plots of different shapes and sizes. Scanning started at plot center by free walking towards the plot border and then by returning to the plot center and forming the closed loop. Depending on the shape and size of plots, as well as on terrain topography, the H-PLS survey lasted between 3 and 9 min per plot.

Another study with simple scanning approach was conducted by Jurjević et al. (2020). Similar to Ryding et al. (2015), they applied a free walking method forming a closed loop by starting and ending the survey at the same point. Data acquisition within the 6 plots ($r=15$ m) was divided into three scanning sessions. A single plot was scanned during the first session, two plots during the second session, and three plots during the third session. The average scanning time per plot was ≈ 4 min including time spent for walking from plot to plot (for the second and third session). To georeference the PCs in post-processing, Jurjević et al. (2020) used spheres (at least three for each session) placed on previously established GCPs and measured using a total station. Therefore, time spent for measuring the positions of spheres was not included in the reported average scanning time.

Del Perugia et al. (2019) evaluated H-PLS scanning approach methods in forest inventory. They investigated the influence of different H-PLS scanning path densities on the estimation of individual tree attributes. Scanning approaches obtained by walking along straight lines with a spacing of 10 m (D10; Fig. 4d – middle) and 15 m (D15; Fig. 4d - right) in circular plots ($r=30$ m) were compared with the reference single-tree scan approach (Fig. 4d – left), which included walking with the H-PLS instrument around each tree. Each scan started and ended at the same point outside the plot forming a closed loop. To georeference PCs, three spherical targets were placed around the plots and their coordinates were acquired using the GNSS receiver. Besides the evaluation of the accuracy of different scanning approaches in the estimation of individual tree attributes, Del Perugia et al. (2019) compared the time spent for data acquisition (scanning) and processing (extraction of individual tree attributes). The average scanning time per plot was 15.0 min, 13.7 min, and 10.3 min for reference single-tree scan, D10 and 15 m scans, respectively. Extraction of individual tree attributes was completed in 55.7 min, 46.7 min and 34.0 min per plot on average for reference single-tree scan, D10 and 15 m scans, respectively. Based on the results obtained (presented in 3.3, 3.4,

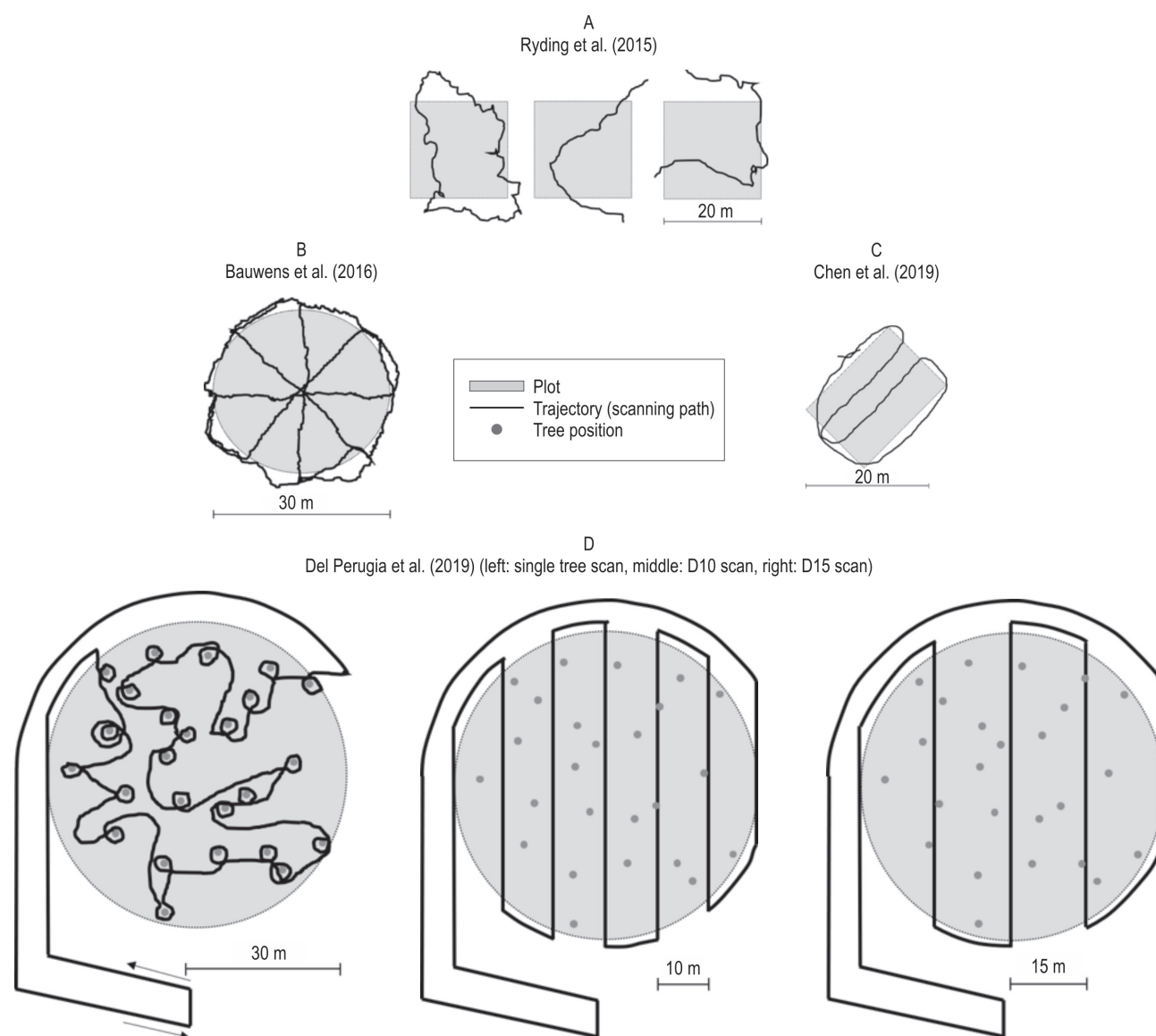


Fig. 4 Examples of trajectories (scanning paths) applied in recent H-PLS studies

3.5), Del Perugia et al. (2019) concluded that D10 scan path provides the best solution, i.e. enables a good balance between acquisition and processing time and accuracy of the results obtained.

In general, all studies emphasized the high time efficiency of H-PLS systems for data collection in forest inventory, where the time spent for H-PLS collection varied between the 3 and 24 min per plot depending on plot size, forest and terrain conditions, and complexity of applied scanning approaches (Ryding et al. 2015, Bauwens et al. 2016, Gianneti et al. 2018, Oveland et al. 2018, Chen et al. 2019, Del Perugia et al. 2019, Gollob et al. 2020, Vantadaşlar and Zeybek 2020).

For example, Gollob et al. (2020) reported 4.7 times faster data acquisition time with H-PLS (10.96 min per plot) than with multi-scan TLS (49.9 min per plot). Furthermore, Bauwens et al. (2016) compared survey time efficiency between different methods and reported survey coverage time per surveyor of $50 \text{ m}^2 \cdot \text{min}^{-1}$, $0.85 \text{ m}^2 \cdot \text{min}^{-1}$ and $0.43 \text{ m}^2 \cdot \text{min}^{-1}$ for H-PLS, TLS and conventional field method, respectively. Similarly, Chen et al. (2019) reported survey coverage time per surveyor of $30 \text{ m}^2 \cdot \text{min}^{-1}$ and $0.81 \text{ m}^2 \cdot \text{min}^{-1}$ for H-PLS and field method, respectively. H-PLS survey included one person and time spent for scanning and pre-processing (automatic registration), while field survey included three persons and time spent for tree species

determination, recording tree location and DBH measurement. Additional time during the field H-PLS survey would be spent if georeferenced PC is needed, i.e. if spherical targets have to be placed and measured in the field using GNSS receiver or total station. The measurement time greatly depends on the availability of the GNSS signal in a particular forest environment.

3.2 Tree Detection

A correct tree segmentation (tree detection) from PCs is the crucial step that directly influences the results and success of the point cloud based forest inventory (Liang et al. 2018a). Successful tree detection using H-PLS depends on many factors, e.g. forest and site conditions, scanning approach, technical characteristics of H-PLS system, applied methodology, etc., and therefore the results obtained among studies can vary (Table 3).

Ryding et al. (2015) and Cabo et al. (2018) compared H-PLS detection rates using multi-scan TLS data with the reported high agreement of 91% and 100%, respectively. High tree detection rates above 90% were also achieved when H-PLS was evaluated with conventional field measurements (Bauwens et al. 2016, Chen et al. 2019, Gollob et al. 2020). The only exception is the study of Oveland et al. (2018) where the detection rate of 76% was reported. In addition to the above-mentioned factors (forest conditions, scanning approach, etc.) influencing the detection rate, the lower DBH threshold (4 cm) applied in Oveland et al. (2018) is also one of the reasons that contributed to the lower detection rate. Out of 87 omitted (non-detected) trees, 68 trees had DBH<10 cm, while the average DBH for all omitted trees was 8.7 cm. This is in line with findings of other H-PLS inventory studies (Ryding et al. 2015, Bauwens et al. 2016, Gianneti et al. 2018) reporting difficulties in segmentation and detection of smaller trees with DBH<10 cm. High beam divergence and low ranging accuracy of used H-PLS instruments and small size of targeted trees result in low point density and high noise of the data, which hinder the tree detection and increase the omission error (Ryding et al. 2015). In general, there have been large variances between reported tree detection accuracy. To date there have been no clear explanations for such big variances between researches, but it can be assumed that differences in forest and site conditions could be one of the main reasons. One possible rationale was pointed out by Hyypä et al. (2020a). In that study, the most important factor limiting the detection of a particular tree was the poor stem visibility due to, e.g., branches and a small stem diameter relates to certain tree species. The pines on the test sites were dominant trees

resulting in detection rate close to 100%. The spruces on the test sites had an occluded stem and a small DBH (average 10 cm), and it was difficult for the applied algorithms to detect the spruce stems and estimate their diameter using the stem detection-based approach employed in Hyypä et al. (2020a). The trees can be found with different algorithm, but estimation of the DBH is challenging from the point cloud data due to occlusions. The occlusions were so bad in Hyypä et al. (2020a), that even human operator could not have estimated the DBH values from the point cloud data.

Based on the obtained results and applied scanning approach, Ryding et al. (2015) concluded that slower walking during scanning and the survey aiming to cover all stems may increase the tree detection rate and reduce omission errors. The importance of scanning approach and resulting scan density on tree detection rate has also been confirmed by Del Perugia et al. (2019). Compared to the reference single-tree scan approach, Del Perugia et al. (2019) achieved considerably higher tree detection rates by applying D10 scan approach (94%) than by D15 scan approach (57%).

Despite the mentioned difficulties to detect the smaller trees, in all studies, high detection rates were achieved for trees with DBH>10 cm. Moreover, several studies showed equivalent performance of H-PLS in tree detection compared to multi-scan TLS (Bauwens et al. 2016, Cabo et al. 2018), and considerably better performance compared to single-scan TLS (Bauwens et al. 2016, Oveland et al. 2018) in more complex forest conditions. In addition, they all emphasized the advantage of using H-PLS over TLS in terms of acquisition and processing time. Promising and even better results were provided by the most recent study of Gollob et al. (2020). Namely, for 20 m radius sample plots and trees with DBH>5 cm, they achieved considerably higher tree detection rates with new H-PLS instrument ZEB-HORIZON (96%) than with multi-scan TLS approach (78%) (Table 3). According to Gollob et al. (2020), the lower number of detected trees with multi-scan TLS occurred because of occlusion effects, where only 4 scans were used. By applying a higher DBH threshold (DBH>10 cm) and plot radii of 20 m, 15 m, and 10 m, detection rates for H-PLS slightly increased to 98.76%, 98.95%, and 99.48%, respectively. However, for TLS detection rates considerably increased by decreasing plot radii and for DBH>10 cm (86.32%, 93.81%, and 98.35%, respectively).

3.3 Tree Position

The accuracy of tree position determined with H-PLS was also evaluated, either with multi-scan TLS as

Table 3 Summary results of tree detection in H-PLS-based forest inventory studies. In comparison studies, the results for other evaluated data (TLS, backpack PLS – B-PLS) are also presented (in grey)

Study	Reference (ground-truth) data	Instrument	DBH threshold of observed trees, cm	Stem density steems · ha ⁻¹	Number of reference trees	Tree detection rate, %
Ryding et al. (2015)	TLS (FARO Focus 3D; 3 scans)	ZEB1	>10	n.a.	54	91
Bauwens et al. (2016)	Conventional field data	ZEB1	>10	113–1344	292	99.5
		TLS (FARO Focus 3D; single scan)	>10	113–1344	292	83
		TLS (FARO Focus 3D; 5 scans)	>10	113–1344	292	99.5
Cabo et al. (2018)	TLS (FARO Focus 3D; 10 scans for site A and 4 scans for site B)	ZEB-REVO	>10	n.a.	271	100
Gianneti et al. (2018)	Conventional field data	ZEB1	>5	106	56	95
		TLS (FARO Focus 3D; 8 scans)	>2.5	106	56	98
Oveland et al. (2018)	Conventional field data	ZEB1	>4	967 (380–1380)	335	74
		TLS (FARO Focus 3D; single scan)	>4	967 (380–1380)	335	62
		B-PLS (in-house-build)	>4	967 (380–1380)	335	88
Chen et al. (2019)	Conventional field data	ZEB-REVO-RT	>5	1100	33	93.3
Del Perugia et al. (2019)	H-PLS (ZEB1; single-tree scan)	ZEB1 (D10)	>5	110	98	94
	H-PLS (ZEB1; single-tree scan)	ZEB1 (D20)	>5	110	98	57
Hyypä et al. (2020a)	TLS (Leica HDS6100; 9 scans for both plots), combined with field measurements	ZEB-HORIZON ^A	>5	410 ^A	42	93
		ZEB-HORIZON ^B	>5	420 ^B	43	77
Gollob et al. (2020)	Conventional field data	ZEB-HORIZON	>5	981 (239–3350)	–	96
		TLS (FARO Focus 3D; 4 scans)	>5	981 (239–3350)	–	78

A Sparse stand
B Obstructed stand

Table 4 Summary results of tree positions in H-PLS-based forest inventory studies. In comparison studies, the results for other evaluated data (TLS, B-PLS) are also presented (in grey)

Study	Reference (ground-truth) data	Instrument	DBH threshold of observed trees, cm	Bias, cm	RMSE cm
Ryding et al. (2015)	TLS (FARO Focus 3D; 3 scans)	ZEB1	<10	2.8	3.9
			>10	1.7	2.1
			All	2.3	3.1
Bauwens et al. (2016)	TLS (FARO Focus 3D; 5 scans)	ZEB1	>10	4.2±7.5	–
		TLS (FARO Focus 3D; single scan)	>10	2.8±14.0	–
Cabo et al. (2018) ^A	TLS (FARO Focus 3D; 10 scans)	ZEB-REVO	>10	–	3.5
Cabo et al. (2018) ^B	TLS (FARO Focus 3D; 4 scans)	ZEB-REVO	>10	–	2.4
Gianneti et al. (2018)	Field data (GNSS receiver for plot center, hypsometer for distance and compass for azimuth to each tree)	ZEB1	>5	2.1	9.3
		TLS (FARO Focus 3D; 8 scans)	>5	2.1	9.3
Oveland et al. (2018)	Field data (GNSS, total station)	ZEB1	>4	17	20
		TLS (FARO Focus 3D; single scan)	>4	69	82
		B-PLS (in-house-build)	>4	54	62
Chen et al. (2019)	Field data (total station)	ZEB-REVO-RT	>5	24	26
Del Perugia et al. (2019)	H-PLS (ZEB1; single-tree scan)	ZEB1 (D10)	>5	–0.001	0.091
	H-PLS (ZEB1; single-tree scan)	ZEB1 (D20)	>5	–0.003	0.139

^A Cabo et al. (2018) – Site A) Urban pine forest (mixed two-aged stand)

^B Cabo et al. (2018) – Site B) Mountain pine forest (even-aged, pure stand)

reference data or field data (Table 4). The results of Ryding et al. (2015) and Cabo et al. (2018) showed high agreement between H-PLS and TLS determined tree positions with RMSE ranging from 2.1 cm to 3.9 cm. In addition, Ryding et al. (2015) achieved higher HPLS position accuracy (RMSE 2.1 cm) for trees with DBH larger than 10 cm than for trees with DBH smaller than 10 cm (RMSE 3.9 cm). High agreement between H-PLS and TLS, i.e. almost identical differences (RMSE=9.3 cm) from tree positions recorded by conventional field survey, were obtained for both datasets by Gianneti et al. (2018). Lower accuracies of H-PLS tree positions evalu-

ated by data from conventional field survey were reported by Oveland et al. (2018) and Chen et al. (2019) with RMSE values of 20.0 cm and 26.0 cm, respectively.

Typically, field measured data is considered as the best available data, however, when using field data as a reference, some additional considerations have to be taken into account. Oveland et al. (2018) reported the standard deviation of 4.5 cm for the field measured tree positions based on the variance of individual errors contributing to uncertainty. The uncertainty of tree position measurements is higher than RMSE reported in most studies that used TLS data as a reference

Table 5 Summary results of DBH estimates in H-PLS-based forest inventory studies. In comparison studies, the results for other evaluated data (TLS, BPLS) are also presented (in grey)

Study	Reference (ground-truth) data	Instrument	DBH threshold cm	Bias cm	Bias %	RMSE cm	RMSE %
Ryding et al. (2015)	TLS (FARO Focus 3D; 3 scans)	ZEB1	<10	1.6	19.5	3.9	46
			>10	-0.9	-5.6	1.5	9
			All	0.3	2.4	2.9	23
Bauwens et al. (2016)	TLS (FARO Focus 3D; 5 scans)	ZEB1	>10	-0.08	-	1.11	4.1
		TLS (FARO Focus 3D; single scan)	>10	-1.17	-	3.73	13.4
		TLS (FARO Focus 3D; 5 scans)	>10	-0.17	-	1.3	4.1
Cabo et al. (2018) ^A	TLS (FARO Focus 3D; 10 scans)	ZEB-REVO	>10	-0.1	-	1.1	-
Cabo et al. (2018) ^B	TLS (FARO Focus 3D; 4 scans)	ZEB-REVO	>10	-0.1	-	0.9	-
Gianneti et al. (2018)	Conventional field data	ZEB1	>5	-0.38	-	1.28	-
		TLS (FARO Focus 3D; 8 scans)	>5	-0.41	-	1.13	-
Oveland et al. (2018)	Conventional field data	ZEB1	>4	0.3	-	3.1	14.3
		TLS (FARO Focus 3D; single scan)	>4	-2.0	-	6.2	28.6
		B-PLS (in-house-build)	>4	0.1	-	2.2	9.1
Chen et al. (2019)	Conventional field data	ZEB-REVO-RT	>5	-1.26	-9.68	1.58	11.88
Zhou et al. (2019)	Conventional field data	Designed ¹	>11.7	0.68 ²	3.45 ²	1.18 ²	-
Gollob et al. (2020)	Conventional field data	ZEB-HORIZON	>5	0.21	1.09	2.32	12.01
		TLS (FARO Focus 3D; 4 scans)	>5	-0.74	-3.83	2.55	13.19
Hyypä et al. (2020a) ^C	TLS (Leica HDS6100; 9 scans for both plots), combined with field measurements	ZEB-HORIZON	>5	-0.4	-1.4	0.9	3.5
Hyypä et al. (2020a) ^D	TLS (Leica HDS6100; 9 scans for both plots), combined with field measurements	ZEB-HORIZON	>5	-0.4	-1.4	1.3	4.2
Vantadaşlar and Zeybek (2020) ³	Conventional field data	ZEB-REVO	>7.9	-	-	-	-

¹ Home-designed H-PLS instrument with integrated Velodyne VLP-16 LiDAR sensor

² Estimated errors correspond to diameter (plane) at 1.2 m from the ground

³ Vantadaşlar and Zeybek (2020) confirmed only high correlation between field and H-PLS measurements ($r=0.97$)

^A Cabo et al. (2018) – Site A) Urban pine forest (mixed two-aged stand)

^B Cabo et al. (2018) – Site B) Mountain pine forest (even-aged, pure stand)

^C Hyypä et al. (2020a) – plot located in sparse stand

^D Hyypä et al. (2020a) – plot located in obscured stand

(Table 2). In general, it is quite difficult to determine the tree position since it is not a distinct point, but an estimate with respect to tree exterior. Positions of the trees with regular geometry of the base (e.g. spruce) can be estimated with higher accuracy than those of the irregular base. Accordingly, different surveyors would estimate different tree positions, whereas algorithms for automated forest inventory would achieve repeatable results every time. In that sense, high accuracy multi-scan TLS data would be a more suitable reference data for tree position assessment than field measurements.

3.4 Diameter at Breast Height

Recent studies (Ryding et al. 2015, Bauwens et al. 2016, Cabo et al. 2018, Gianneti et al. 2018, Oveland et al. 2018, Chen et al. 2019, Zhou et al. 2019., Gollob et al. 2020, Hyypä et al. 2020a, Vantadaşlar and Zeybek 2020) revealed that H-PLS also provides accurate DBH estimates from properly segmented and detected trees (Table 5). In these studies, DBH was usually estimated by fitting point cloud slice at 1.3 m with circle, ellipse or cylinder. Chen et al. (2019) calculated DBH from polygonal cylindrical volume. Regardless of the fitting method, a high agreement between H-PLS estimates and reference data (multi-scan TLS or field DBH) were reported in most studies (Ryding et al. 2015, Bauwens et al. 2016, Cabo et al. 2018, Gianneti et al. 2018, Oveland et al. 2018, Chen et al. 2019) with RMSE values ranging from 0.9 cm to 1.58 cm, with the exception of the studies where smaller trees (DBH<10 cm) were included in the DBH estimation (Ryding et al. 2015, Oveland et al. 2018, Gollob et al. 2020) with RMSE values ranging from 2.3 cm to of 3.1 cm. Furthermore, Ryding et al. (2015) obtained considerably greater errors for trees with DBH<10 cm (RMSE of 3.9 cm or 46%) than for trees with DBH>10 cm (RMSE of 1.5 cm or 9%). The reasons of lower accuracy of DBH estimates for smaller trees using H-PLS are the same as for tree detection and tree position elaborated previously, i.e. high beam divergence and low ranging accuracy of H-PLS instruments, the small size of targeted trees which results in point clouds of relatively low density and high noise. The influence of noise on the DBH estimation was reported by Gollob et al. (2020) as well. Due to high noise in H-PLS PC, DBH of small trees (DBH<10 cm) was constantly overestimated regardless of various fitting methods applied. With increased noise and decreased DBH, overestimation increased. Applied scanning approach and forest characteristics (e.g. stem density, presence of understory) can also considerably influence the results, in both positive or negative directions. In Hyypä et al.

(2020a), temporal filtering and novel post-SLAM-correction were applied resulting in high-quality DBH values, similarly to Hyypä et al. (2020b).

The general conclusion from the recent studies, mostly based on a relatively small sample, showed the ability of H-PLS to successfully extract and estimate DBH (especially for trees with DBH>10 cm) with similar performance to multi-scan TLS or field measurements. Moreover, in comparison studies of Oveland et al. (2018) and Gollob et al. (2020), where smaller trees were also included, H-PLS estimated DBH with higher accuracy than multi-scan TLS data (Table 5). However, these results have to be taken with caution due to a limited number of conducted H-PLS studies, which prevents formulating a clear understanding and interpretation of the results at present.

3.5 Tree Height

Along with DBH, tree height is one of the fundamental measurements in forest inventories, either in operational or national inventories. It is often used to calculate individual tree, plot or stand attributes (e.g. volume, biomass, carbon stock, stand growth and productivity, site index, etc.). Therefore, the accuracy of tree height estimates directly influences the accuracy of other derivative, i.e. indirectly measured, inventory attributes (Feldpausch et al. 2012, Wang et al. 2019).

Despite the importance of the tree height variable, the accuracy of tree height estimation using H-PLS was studied in only a few studies up to now (Cabo et al. 2018, Gianneti et al. 2018, Jurjević et al. 2020, Hyypä et al. 2020a) (Table 6). It is assumed that the main reason for that was the limited scanning range of the first commercial H-PLS instruments that have been mostly used in recent studies. Namely, for ZEB1, ZEB-REVO and ZEB-REVO-RT, the manufacturer declared the range of 30 m and 15-20 m for indoors and outdoors, respectively (GEOSLAM 2017).

This limitation of first H-PLS instruments was confirmed by Cabo et al. (2018) and Gianneti et al. (2018), who reported that tree height estimation of taller trees is considerably hindered by limited scanning range of the laser. Cabo et al. (2018) conducted a comparison study between multi-scan TLS and H-PLS at two sites. While TLS and H-PLS heights achieved a good agreement (RMSE=1.34 m) in the first site of urban pine forest mostly consisting of trees lower than 20 m, a high disagreement (RMSE=9.44 m) between TLS and H-PLS heights was reported for the second site of mountain pine forest with most of the trees higher than 20 m. Furthermore, Cabo et al. (2018) evaluated the accuracy of H-PLS tree height estimates for all trees at both sites in comparison to TLS data, as well as for three data

subsets: trees with heights estimated from TLS lower than 10 m, 9 m, and 8 m. For all the trees, including both test sites, the RMSE was 3.79 m. For trees lower than 10 m, 9 m, and 8 m, the RMSE values were 0.74 m, 0.73 m, and 0.65 m, respectively. This research showed that in comparison to TLS, tree heights estimated using H-PLS instruments with limited scanning range produced greater errors and greater underestimations with increasing the tree height. The errors considerably increase when tree heights are higher than the maximum scanning range of the H-PLS instrument.

The underestimation of tree heights using H-PLS was reported by Giannetti et al. (2018), as well. Despite the relatively lower tree heights in the study area (12.5 m on average), H-PLS underestimated tree heights with a bias of -4.61 m and RMSE of 2.15 m in comparison to field reference data.

To the best of authors' knowledge, the studies of Jurjević et al. (2020) and Hyypä et al. (2020a) are the first and so far the only that used a new generation of commercial H-PLS instruments (ZEB-HORIZON) with considerably improved features of LiDAR sensor (scanning range and acquisition rate) for tree height estimation. In a comparison study that encompassed field data and various close-range remote sensing data (PLS, ULS, UAV), Jurjević et al. (2020) obtained promising results. Compared to field tree height measurements, PLS achieved the highest accuracy (RMSE=4.45%, $r=0.98$), followed by ULS (RMSE=5.33%, $r=0.98$) and UAV (RMSE=5.94%, $r=0.97$). Unlike in studies (Cabo et al. 2018, Giannetti et al. 2018), where H-PLS of limited scanning range were used and considerably underestimated tree heights, in Jurjević et al. (2020) H-PLS tree heights were slightly overestimated (Bias=1.82%). These results are important since most of

Table 6 Summary results of tree height estimates in H-PLS-based forest inventory studies. In comparison studies, the results for other evaluated data (TLS, ULS, UAV) are also presented (in grey)

Study	Reference (ground-truth) data	Instrument	Tree height range, m ¹	Bias, m	RMSE, m
Cabo et al. (2018) ^A	TLS (FARO Focus 3D; 10 scans)	ZEB-REVO	≈5–18	0.94±0.96	1.34
Cabo et al. (2018) ^B	TLS (FARO Focus 3D; 4 scans)	ZEB-REVO	≈21–33	9.03±2.76	9.44
Cabo et al. (2018) ^{A+B}	TLS (FARO Focus 3D; 10 and 4 scans)	ZEB-REVO	≈5–33	2.79±2.95	3.79
			≈5–10	0.21±0.71	0.74
			≈5–9	0.14±0.72	0.73
			≈5–8	-0.06±0.66	0.65
Giannetti et al. (2018)	Conventional field data	ZEB1	≈2–19	-4.61	2.15
		TLS (FARO Focus 3D; 8 scans)	≈2–19	-0.61	0.88
Hyypä et al. (2020a) ²	Conventional field data	ZEB-HORIZON	7–28	-0.16; -1.1	0.4; 1.4
		B-PLS	7–28	1.4; 0.55	1.5; 1.0
		UAV/Ricopiter	7–28	0.0; 0.8	0.82; 1.6
Jurjević et al. (2020)	Conventional field data	ZEB-HORIZON	≈9–33	0.45	1.11
		ULS	≈9–33	0.62	1.38
		UAV	≈9–33	0.88	1.58

A Site A) Urban pine forest (mixed two-aged stand)

B Site B) Mountain pine forest (even-aged, pure stand)

1 For the study of Cabo et al. (2018) and Giannetti et al. (2018) tree height range was estimated from presented data (graphs)

2 For the study of Hyypä et al. (2020a) the first values of Bias and RMSE are for the plot located in sparse stand and the second values are for the plot located in obscured stand

C Hyypä et al. (2020a) – plot located in sparse stand

D Hyypä et al. (2020a) – plot located in obscured stand

the trees in the study area are considerably taller than trees in other studies (Cabo et al. 2018, Gianneti et al. 2018). Namely, the average heights of the main tree species in the study area were 28.88 m, 20.04 m, 19.91 m, and 17.79 m for pedunculate oak (71 trees), common hornbeam (45 trees), black alder (6 trees), and others (8 trees), respectively. In a forthcoming paper (Hyypä et al. 2020a), six emerging MLS technologies were compared for field reference data collection at the individual tree level in boreal forest conditions, namely an in-house developed AKHKA-R3 B-PLS, a ZEB-HORIZON H-PLS, an under-canopy ULS, and three above-canopy ULS. Concerning canopy height, it was observed that the B-PLS and the H-PLS could be used for sufficiently accurate tree height measurements (RMSE=2–10%). Hyypä et al. (2020a) concluded that the accuracy of the MLS-based tree heights coincide with the tree heights estimated from above-canopy laser scanning measurements in medium-difficult boreal forest conditions. Hyypä et al. (2020a) concluded that the ZEB-HORIZON H-PLS underestimated the heights of trees above 25 m, and should not be used to measure the heights of trees much taller than 25 m.

Meanwhile, one should keep in mind that accuracy of indirect field tree height measurements can be influenced by a number of potential errors (e.g. forest structure and complexity, tree species and tree crown shape, tree height, leaning trees, topography, measuring distance, instrument and human errors, etc.) (Bragg 2014, Sterenczak et al. 2019). Therefore, the errors of the tree height accuracy from H-PLS include both H-PLS and reference related errors when using field measured tree heights as a reference. Lately, Wang et al. (2019) proved that high density airborne laser measurement provide more reliable tree height estimates than the conventional field measurements.

4. Discussion and Outlook

A significant advantage of H-PLS is the light weight and size resulting in high mobility, and consequently high efficiency in data acquisition. All comparison studies dealing with the acquisition time (Bauwens et al. 2016, Chen et al. 2019, Gollob et al. 2020) emphasized the high time efficiency of H-PLS systems in forest inventory, compared to conventional field measurements and especially to multi-scan TLS surveys. However, while widely expected to solve the occlusion effects present in TLS by roaming forest area, H-PLS still have the occlusion problem according to the previous studies, especially in complicated forest conditions (e.g. high stem density, dense understorey) similar to TLS. Ryding et al. (2015) emphasized

that the omission errors can be caused by point occlusion within the point cloud, which especially occurs in areas of high stem density and increased understorey. This emphasizes the essence of the impact of path planning on successful data acquisition.

Lightweight laser sensors are under continuous improvement at the moment due to the driving forces in autonomous driving and general robotics. The scanning range of H-PLS has been clearly improved lately. Early studies with H-PLS (Cabo et al. 2018, Gianneti et al. 2018) did not report promising results regarding the tree height estimation. The reported errors considerably increased when tree heights were higher than the maximum scanning range of the H-PLS instrument (15–20 m). The scanning range of the recent commercial H-PLS instrument has been considerably improved, e.g. up to 100 m, and the recent study has shown the potential to estimate tree height (Jurjević et al. 2020); however, canopy height higher than 25 m are underestimated in some conditions (Hyypä et al. 2020a). In general, H-PLS is still at an early development stage, and has lots of potential for the future. Technical improvements and new systems could be expected to emerge, as there are a half a dozen sensor manufacturers with a plethora of laser scanners models suitable for H-PLS.

H-PLS relies on SLAM algorithms to build the point cloud. Current SLAM methods contain noticeable errors, as shown by clear point distribution variances on planar surfaces, (e.g. Ryding et al. 2015). While previous works mostly showed that the current SLAM works in different forest conditions, Bauwens et al. (2016) reported that H-PLS completely failed in forest areas with high stem density and dense understorey as well as in areas with low stem density, these being the only two cases so far in which H-PLS and SLAM meet problems in forest conditions. Further research needs to be carried out in various forest conditions with larger samples (e.g. number of plots) in order to give more information on the applicability of the SLAM solution in forest conditions. Nevertheless, artifacts caused by misregistration of the scans can be found even in the forest areas of the moderate stem density and understorey (Fig. 5). The effect of this error depends primarily on the robustness of the algorithm that is used for attribute extraction. Fig. 5 shows the scan misregistration effect forming a »shadow« of the recorded tree.

Laser sensors in HPLS are typically less expensive than TLS, integrated systems are currently at the same price range or even more expensive however, and have lower ranging accuracies and angular resolutions and larger beam divergences and footprints. Consequently,

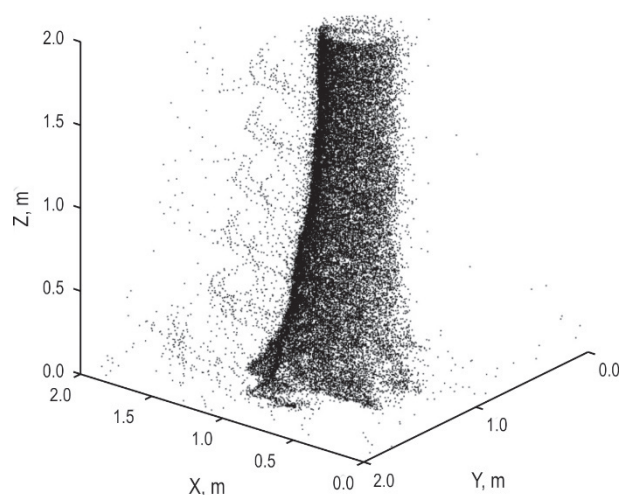


Fig. 5 SLAM misregistration effect

H-PLS data quality, e.g. geometric accuracy, and point density, is lower and the level of noise is higher in comparison to TLS. H-PLS is expected to be suitable for retrieving tree stem attributes in mature forest and to have difficulties to record and consequently to detect and model small trees (DBH<10 cm). The challenges that H-PLS has in modeling trees in small size have been reported in most of the recent studies (Ryding et al. 2015, Bauwens et al. 2016, Gianneti et al. 2018, Oveland et al. 2018, Chen et al. 2019, Gollob et al. 2020).

Meanwhile, the quality of H-PLS data is also affected by the operator's walking speed during data acquisition. Low speed has been suggested to have positive effects on the data quality (Ryding et al. 2015, Del Perugia et al. 2018), while it also means long acquisition time and higher survey costs. All mentioned factors have to be considered when planning an efficient H-PLS survey. Up to now, different walking patterns, speeds and their combinations have been tested in previous studies. However, no protocol has been established for field data acquisition. The best practices of H-PLS data acquisition needs to be further investigated to establish practical guide for successful field work.

In general, previous studies reported that individual tree attributes, i.e. tree detection, tree position and DBH, were estimated with high accuracy using H-PLS. For the DBH estimates, the RMSE value reported was 1.28 cm in Gianneti et al. (2018), 3.1 cm in Oveland et al. (2018), 1.58 cm in Chen et al. (2019), 2.32 cm in Gollob et al. (2020) for trees larger than 4 or 5 cm. These results were at the same level or close to those achieved in the DBH estimates, i.e. less than 2 cm, in three forest complexity categories using multi-scan TLS (Liang et

al. 2018a). In addition, almost identical results were reported when using H-PLS and multi-scan TLS evaluated by conventional ground reference. In Gianneti et al. (2018), RMSE was reported as 1.28 cm and 1.13 cm for H-PLS and TLS, respectively. In Gollob et al. (2020), RMSE was reported as 2.32 cm and 2.55 cm.

For the tree detection, the completeness reported was 95% in Gianneti et al. (2018), 74% in Oveland et al. (2018), 93% in Chen et al. (2019), 96% in Gollob et al. (2020). Most of these results were above 90%, and close or even a bit higher than what at best can be achieved in easy and medium forests using multi-scan TLS, and approximately 30% higher than multi-scan TLS in difficult forests.

These results, on the one hand, have shown the potential of the application of H-PLS systems in forest inventory. On the other hand, the reported results may be optimistic considering the technical challenges that H-PLS has, and may not yet fully reveal the limiting factors in the application of H-PLS.

5. Conclusion

Lightweight laser scanners have experienced rapid technological progress in recent years. They can be easily mounted on various unmanned aerial and static or mobile (car, all-terrain vehicle, human) terrestrial platforms and have the potential to provide detailed information on forests and consequently have the possibility to extract information at individual tree level. Among all these systems, H-PLS is the most recent development. With the emergence of a few commercial H-PLS systems in the market in the last few years, research has started to study the feasibility of individual tree attributes estimation, e.g. tree detection, tree position, DBH, tree height, and to evaluate its performance with conventional field measurements or multi-scan TLS data. While the reported studies showed some promising results, given the limited number of conducted studies, it is not yet possible to conclude whether H-PLS systems are currently suitable for operational forest inventory. More research is required in order to provide any recommendation for practice. Further research should focus on establishing protocol for field data acquisition, clarifying the occlusion effects and completeness of the data, and revealing the performance in varying forest conditions.

Acknowledgments

This research was funded by projects »Retrieval of Information from Different Optical 3D Remote Sensing Sources for Use in Forest Inventory (3D-FORINVENT)«

funded by the Croatian Science Foundation (HRZZ IP-2016-06-7686) and »Operational Sustainable Forestry with Satellite-Based Remote Sensing (My Sustainable Forest)« funded by the the European Union's Horizon 2020 research and innovation programme under grant agreement No 776045. Xinlian Liang, Juha Hyyppä, Antero Kukko would like to thank Academy of Finland for the financial supports to conduct this research through projects 334829, 331708, 300066, and 334002. The work of doctoral student Luka Jurjević has been supported in part by the »Young researchers' career development project – training of doctoral students« of the Croatian Science Foundation funded by the European Union from the European Social Fund. Part of Luka Jurjević's work was completed during his visiting to Finnish Geospatial Research Institute and Centre of Excellence in Laser Scanning Research.

6. References

- Bauwens, S., Bartholomeus, H., Calders, K., Lejeune, P., 2016: Forest inventory with terrestrial LiDAR: A comparison of static and hand-held mobile laser scanning. *Forests* 7(6): 127. <https://doi.org/10.3390/f7060127>
- Bragg, D.C., 2014: Accurately measuring the height of (real) forest trees. *Journal of Forestry* 112(1): 51–54. <https://doi.org/DOI:10.5849/jof.13-065>
- Cabo, C., Del Pozo, S., Rodríguez-González, P., Ordóñez, C., González-Aguilera, D., 2018: Comparing terrestrial laser scanning (TLS) and wearable laser scanning (WLS) for individual tree modeling at plot level. *Remote Sens.* 10(4): 540. <https://doi.org/10.3390/rs10040540>
- Chen, S., Liu, H., Feng, Z., Shen, C., Chen, P., 2019: Applicability of personal laser scanning in forestry inventory. *PLoS ONE* 14(2): e0211392. <https://doi.org/doi:10.1371/journal.pone.0211392>
- Del Perugia, B., Giannetti, F., Chirici, G., Travaglini, D., 2019: Influence of scan density on the estimation of single-tree attributes by hand-held mobile laser scanning. *Forests* 10(3): 277. <https://doi.org/10.3390/f10030277>
- Feldpausch, T.R., Lloyd, J., Lewis, S.L., Brien, R.J., Gloor, M., Monteagudo Mendoza, A., Lopez-Gonzalez, G., Banin, L., Abu Salim, K., Affum-Baffoe, K., Alexiades, M., 2012: Tree height integrated into pantropical forest biomass estimates. *Biogeosciences* 9(8): 3381–3403. <https://doi.org/10.5194/bg-9-3381-2012>
- GEOSLAM. Available online: <https://geoslam.com/> (accessed 1 March 2020)
- Giannetti, F., Puletti, N., Quatrini, V., Travaglini, D., Bottalico, F., Corona, P., Chirici, G., 2018: Integrating terrestrial and airborne laser scanning for the assessment of single-tree attributes in Mediterranean forest stands. *Eur. J. Remote Sens.* 51(1): 795–807. <https://doi.org/10.1080/22797254.2018.1482733>
- Gollob, C., Ritter, T., Nothdurft, A., 2020: Forest Inventory with Long Range and High-Speed Personal Laser Scanning (PLS) and Simultaneous Localization and Mapping (SLAM) Technology. *Remote Sens.* 12(9): 1509. <https://doi.org/10.3390/rs12091509>
- Hyyppä, J., Jaakkola, A., Chen, Y., Kukko, A., 2013: Unconventional LIDAR mapping from air, terrestrial and mobile. In *Proceedings of the Photogrammetric Week*; Wichmann/VDE Verlag: Berlin, Germany; 205–214 p.
- Hyyppä, E., Yu, X., Kaartinen, H., Hakala, T., Kukko, A., Vastaranta, M., Hyyppä, J., 2020a: Comparison of Backpack, Handheld, Under-Canopy UAV, and Above-Canopy UAV Laser Scanning for Field Reference Data Collection in Boreal Forests. *Remote Sens.* 12(20): 3327. <https://doi.org/10.3390/rs12203327>
- Hyyppä, E., Hyyppä, J., Hakala, T., Kukko, A., Wulder, M.A., White, J.C., Pyörälä, J., Yu, X., Wang, Y., Virtanen, J.P., Pohjavirta, O., Liang, X., Holopainen, M., Kaartinen, H., 2020b: Under-canopy UAV laser scanning for accurate forest field measurements. *ISPRS J. Photogramm. Remote Sens.* 164: 41–60. <https://doi.org/10.1016/j.isprsjprs.2020.03.021>
- Jurjević, L., Liang, X., Gašparović, M., Balenović, I., 2020: Is field-measured tree height as reliable as believed – Part II, A comparison study of tree height estimates from conventional field measurement and low-cost close-range remote sensing in a deciduous forest. *ISPRS J. Photogramm. Remote Sens.* 169: 227–241. <https://doi.org/10.1016/j.isprsjprs.2020.09.014>
- Kukko, A., Kaartinen, H., Hyyppä, J., Chen, Y., 2012: Multi-platform mobile laser scanning: Usability and performance. *Sensors* 12(9): 11712–11733. <https://doi.org/10.3390/s120911712>
- Liang, X., Hyyppä, J., Kaartinen, H., Holopainen, M., Melkas, T., 2012: Detecting changes in forest structure over time with bi-temporal terrestrial laser scanning data. *ISPRS Int. J. Geo-Inf.* 1(3): 242–255. <https://doi.org/10.3390/ijgi1030242>
- Liang, X., Kankare, V., Xiaowei, Y., Hyyppä, J., Holopainen, M., 2014: Automated Stem Curve Measurement Using Terrestrial Laser Scanning. *IEEE Trans. Geosci. Remote Sens.* 52(3): 1739–1748. <https://doi.org/10.1109/TGRS.2013.2253783>
- Liang, X., Hyyppä, J., Kaartinen, H., Lehtomäki, M., Pyörälä, J., Pfeifer, N., Holopainen, M., Brolly, G., Francesco, P., Hackenberg, J., Huang, H., Jo, H.-W., Katoh, M., Liu, L., Mokroš, M., Morel, J., Olofsson, K., Poveda-Lopez, J., Trochta, J., Wang, D., Wang, J., Xi, Z., Yang, B., Zheng, G., Kankare, V., Luoma, V., Yu, X., Chen, L., Vastaranta, M., Saarinen, N., Wang, Y., 2018a: International benchmarking of terrestrial laser scanning approaches for forest inventories. *ISPRS J. Photogramm. Remote Sens.* 144: 137–179. <https://doi.org/10.1016/j.isprsjprs.2018.06.021>
- Liang, X., Kukko, A., Hyyppä, J., Lehtomäki, M., Pyörälä, J., Yu, X., Kaartinen, H., Jaakkola, A., Wang, Y., 2018b: In-situ measurements from mobile platforms: An emerging approach to address the old challenges associated with forest inventories. *ISPRS J. Photogramm. Remote Sens.* 143: 97–107. <https://doi.org/10.1016/j.isprsjprs.2018.04.019>

- Næsset, E., 2014: Area-Based Inventory in Norway – From Innovation to an Operational Reality. In *Forestry Applications of Airborne Laser Scanning. Managing Forest Ecosystems*; Maltamo, M., Næsset, E., Vauhkonen, J., Eds.; Springer, Dordrecht, The Netherlands, 27; 215–240. https://doi.org/10.1007/978-94-017-8663-8_11
- Ørka, H.O., Bollandsås, O.M., Hansen, E.H., Næsset, E., Gobakken, T., 2018: Effects of terrain slope and aspect on the error of ALS-based predictions of forest attributes. *Forestry* 91(2): 225–237. <https://doi.org/10.1093/forestry/cpx058>
- Oveland, I., Hauglin, M., Giannetti, F., Schipper Kjørsvik, N., Gobakken, T., 2018: Comparing three different ground based laser scanning methods for tree stem detection. *Remote Sens.* 10(4): 538. <https://doi.org/10.3390/rs10040538>
- Petrie, G., Toth, C.K., 2009: Introduction to Laser Ranging, Profiling and Scanning. In *Topographic Laser Ranging and Scanning: Principles and Processing*; Shan, J., Toth, C.K., Eds.; CRC Press/Taylor & Francis, London, England, UK, 1–28. <https://doi.org/10.1201/9781420051438>
- Ryding, J., Williams, E., Smith, M.J., Eichhorn, M.P., 2015: Assessing handheld mobile laser scanners for forest surveys. *Remote Sensing* 7(1): 1095–1111. <https://doi.org/10.3390/rs70101095>
- Stereńczak, K., Mielcarek, M., Wertz, B., Bronisz, K., Zajączkowski, G., Jagodziński, A.M., Ochał, W., Skorupski, M., 2019: Factors influencing the accuracy of ground-based tree-height measurements for major European tree species. *J. Environ. Manage.* 231: 1284–1292. <https://doi.org/10.1016/j.jenvman.2018.09.100>
- Tuominen, S., Pitkänen, J., Balazs, A., Korhonen, K.T., Hyvönen, P., Muinonen, E., 2014: NFI plots as complementary reference data in forest inventory based on airborne laser scanning and aerial photography in Finland. *Silva Fenn.* 48(2): 983. <https://doi.org/10.14214/sf.983>
- Vatandaşlar, C., Zeybek, M., 2020: Application of handheld laser scanning technology for forest inventory purposes in the NE Turkey. *Turkish Journal of Agriculture and Forestry* 44(3): 229–242. <https://doi.org/10.3906/tar-1903-40>
- Wang, Y., Lehtomäki, M., Liang, X., Pyörälä, J., Kukko, A., Jaakkola, A., Liu, J., Feng, Z., Chen, R., Hyyppä, J., 2019: Is field-measured tree height as reliable as believed—A comparison study of tree height estimates from field measurement, airborne laser scanning and terrestrial laser scanning in a boreal forest. *ISPRS J. Photogramm. Remote Sens.* 147: 132–145. <https://doi.org/10.1016/j.isprsjprs.2018.11.008>
- White, J.C., Coops, N.C., Wulder, M.A., Vastaranta, M., Hilker, T., Tompalski, P., 2016: Remote Sensing Technologies for Enhancing Forest Inventories: A Review. *Can. J. Remote Sens.* 42(5): 619–641. <https://doi.org/10.1080/07038992.2016.1207484>
- Zhou, S., Kang, F., Li, W., Kan, J., Zheng, Y. He, G., 2019: Extracting diameter at breast height with a handheld mobile LiDAR system in an outdoor environment. *Sensors* 19(14): 3212. <https://doi.org/10.3390/s19143212>



© 2020 by the authors. Submitted for possible open access publication under the terms and conditions of the Creative Commons Attribution (CC BY) license (<http://creativecommons.org/licenses/by/4.0/>).

Authors' addresses:

Ivan Balenović, PhD
e-mail: ivanb@sumins.hr
Croatian Forest Research Institute
Division for Forest Management and Forestry Economics
Trnjanska cesta 35
10450 Zagreb
CROATIA

Xinlian Liang, D.Sc. (Tech.)
e-mail: xinlian.liang@nls.fi
Finnish Geospatial Research Institute, FGI
Department of Remote Sensing and Photogrammetry
Geodeetinrinne 2
02430 Masala
FINLAND

Luka Jurjević, mag. ing. geod. et geoinf. *
e-mail: lukaj@sumins.hr
Croatian Forest Research Institute
Division for Forest Management and Forestry Economics
Trnjanska cesta 35
10450 Zagreb
CROATIA

Prof. Juha Hyyppä, D.Sc. (Tech.)
e-mail: juha.hyyppa@nls.fi
Finnish Geospatial Research Institute, FGI
Department of Remote Sensing and Photogrammetry
Geodeetinrinne 2
02430 Masala
FINLAND

Prof. Ante Seletković, PhD
e-mail: aseletkovic@sumfak.hr
University of Zagreb
Faculty of Forestry
Department of Forest Inventory and Management
Svetošimunska 25
10000 Zagreb
CROATIA

Prof. Antero Kukko, D.Sc. (Tech.)
e-mail: antero.kukko@nls.fi
Finnish Geospatial Research Institute, FGI
Department of Remote Sensing and Photogrammetry
Geodeetinrinne 2
02430 Masala
FINLAND

* Corresponding author

Received: March 16, 2020
Accepted: July 16, 2020